

SCIENTIFIC REPORTS

OPEN

Compound-specific $\delta^{15}\text{N}$ composition of free amino acids in moss as indicators of atmospheric nitrogen sources

Ren-guo Zhu^{1,2}, Hua-Yun Xiao^{1,2}, Zhongyi Zhang^{1,2} & Yuanyuan Lai^{1,3}

Haplocladium microphyllum moss samples were collected in Nanchang, China. Free amino acid (FAA) concentrations and N isotope compositions ($\delta^{15}\text{N}_{\text{FAA}}$) in the samples were determined and compared with the bulk N concentrations and $\delta^{15}\text{N}_{\text{bulk}}$ values. The aim was to determine whether $\delta^{15}\text{N}_{\text{FAA}}$ values in moss (which are very variable) indicate the sources of atmospheric N. The $\delta^{15}\text{N}_{\text{FAA}}$ values among individual FAA varied widely (from -19.3‰ to $+16.1\text{‰}$), possibly because of the different sources of N and isotope fractionation in amino acids metabolic pathways. Total ^{15}N -enrichment for the individual FAAs was equal to total ^{15}N -depletion relative to $\delta^{15}\text{N}_{\text{bulk}}$. The concentration-weighted mean $\delta^{15}\text{N}$ value for total FAAs (TFAA) ($\delta^{15}\text{N}_{\text{TFAA}}$) was $-3.1\text{‰} \pm 3.2\text{‰}$, which was similar to $\delta^{15}\text{N}_{\text{bulk}}$ ($-4.0\text{‰} \pm 2.9\text{‰}$). We concluded that a N isotope balance occurred during amino acid metabolism and that little isotope disparity occurred between the concentration-weighted TFAA and bulk N. We concluded that $\delta^{15}\text{N}_{\text{TFAA}} \approx \delta^{15}\text{N}_{\text{bulk}} \approx \delta^{15}\text{N}_{\text{source}}$. The mean $\delta^{15}\text{N}_{\text{alanine}}$ (-4.1‰), $\delta^{15}\text{N}_{\text{glutamate}}$ (-4.2‰), and $\delta^{15}\text{N}_{\text{lysine}}$ (-4.0‰) were similar to the mean $\delta^{15}\text{N}_{\text{bulk}}$, which we attributed to little isotope fractionation occurring during their *in situ* the metabolic pathways. This suggests that $\delta^{15}\text{N}_{\text{alanine}}$, $\delta^{15}\text{N}_{\text{glutamate}}$, and $\delta^{15}\text{N}_{\text{lysine}}$ in moss can be used to indicate the sources of atmospheric N deposition.

Anthropogenic N pollution entering the atmosphere is increasing every year¹. It is predicted that global anthropogenic N emissions will be 200 Tg y^{-1} by 2050². Atmospheric N deposition can influence soil chemistry³, lacustrine and estuarine eutrophication⁴, biological diversity⁵, greenhouse gas balance⁶, and even human health⁷. The levels and sources of atmospheric N deposition urgently need to be assessed.

Due to lack protective cuticles and have large surface areas, moss receives N passively and effectively from atmospheric N deposition^{8–11}. Mosses have therefore been used widely to easily and cheaply acquire relatively high spatial resolution data on long-term atmospheric N deposition. Strong relationships between atmospheric N deposition and bulk N concentrations in moss tissues have been found in numerous studies^{12–17}.

In field studies, FAA has been found to be more sensitivity to atmospheric N deposition than bulk N in moss^{18,19}. Laboratory experiments using ^{15}N labelled compounds have indicated that N-containing compounds taken up by moss are immediately assimilated as glutamine (Gln) and then transformed into other FAAs to avoid toxic NH_4^+ concentrations accumulating in the cells^{20,21}. Strong links between the concentrations of some FAAs and atmospheric N deposition have been found for vascular plants^{18,22–27}. However, different types of FAAs have been found to accumulate in different plant species^{25,28}. It is still unclear whether FAA concentrations in moss can be used to quantitatively indicate N deposition and which specific FAAs respond most to atmospheric N deposition.

Moss depends on atmospheric N deposition as its main N source and the low isotopic fractionation is accompanied with the uptake of N by moss^{13,29,30}. Bulk N isotope compositions ($\delta^{15}\text{N}_{\text{bulk}}$) in moss have therefore been used to indicate the dominant sources of N deposition^{31–36}. For example, $\delta^{15}\text{N}_{\text{bulk}}$ for moss has been found to significantly negatively correlate with the wet deposition $\text{NH}_4^+/\text{NO}_3^-$ ratio^{27,37}. However, influences of atmospheric

¹Jiangxi Province Key Laboratory of the Causes and Control of Atmospheric Pollution, East China University of Technology, Nanchang, 330013, China. ²College of Water Resources and Environmental Engineering, East China University of Technology, Nanchang, 330013, China. ³College of Earth Sciences, East China University of Technology, Nanchang, 330013, China. Correspondence and requests for materials should be addressed to H.-Y.X. (email: xiaohuayun@ecit.cn)

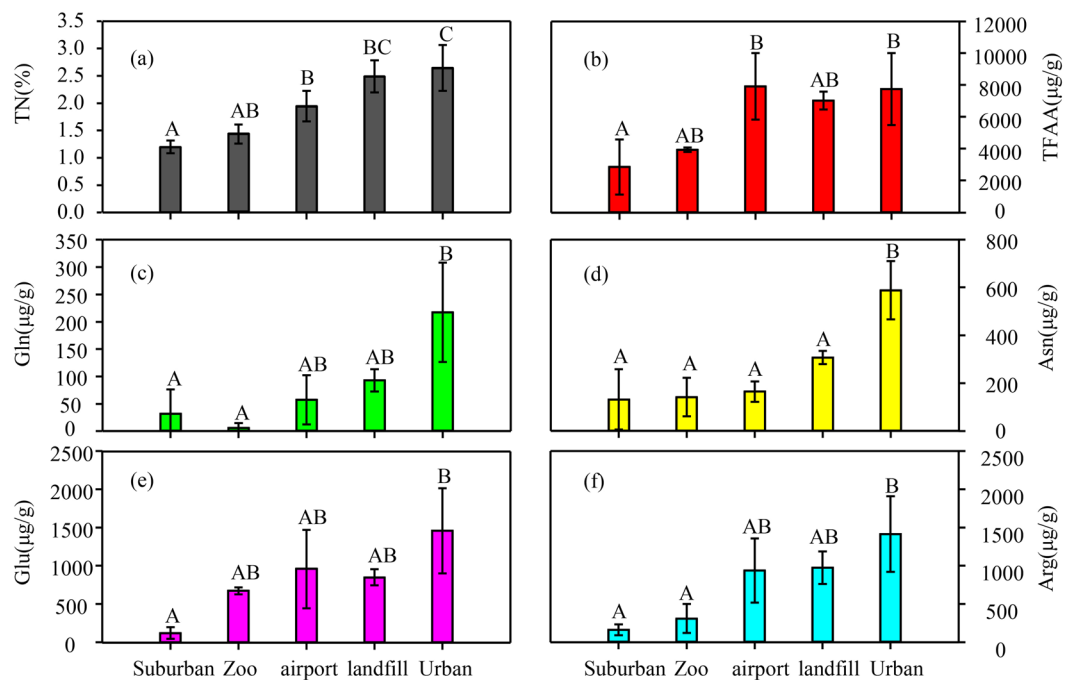


Figure 1. Concentrations of TN, TFAA, Gln, Asn, Glu and Arg in moss from Suburban, Zoo, Airport, Landfill and Urban in Nanchang city: (a) TN, (b) TFAA, (c) Gln, (d) Asn, (e) Glu and (f) Arg. Bars represent mean values \pm standard deviations. Significantly different mean values (HSD Tukey's, $p < 0.05$) of TN and FAA from different sampling sites are indicated with superscript letters 'A' and 'B'.

N deposition on N utilization and metabolism of moss were hindered by only analyzing the $\delta^{15}\text{N}_{\text{bulk}}$ ^{38,39}. FAAs are important N-containing biomolecules that play central roles in N metabolism in plants and have been shown to be sensitive to atmospheric N pollution⁴⁰. FAA $\delta^{15}\text{N}$ values can be used to help evaluate the responses of N metabolism in plants to environmental N inputs. Bol, *et al.*⁴¹ found that the histidine (His) and phenylalanine (Phe) $\delta^{15}\text{N}$ values can be used to differentiate functional strategy in relative to acquisition of available N sources. Xu and Xiao⁴² found that the $\delta^{15}\text{N}$ values of some FAAs and total FAAs (TFAA) in needles were depleted when the contribution of traffic was lower. However, Yoneyama and Tanaka⁴³ found that a significant isotopic fractionation was connected to the metabolism of FAA in plants. In previous studies differences between $\delta^{15}\text{N}_{\text{FAA}}$ values among individual FAA up to 36‰ have been found^{38,42}. However, no study explore how $\delta^{15}\text{N}_{\text{FAA}}$ pattern reflects atmospheric N source when strong isotope fractionation occurs through FAA metabolism and which specific FAA best reflect the isotope signatures of atmospheric N sources in moss has yet been performed. It is therefore necessary to investigate the relationship between ^{15}N abundances in individual FAAs and atmospheric N sources.

In this study, we determined the FAA N concentrations, $\delta^{15}\text{N}_{\text{FAA}}$ values, bulk N concentrations and $\delta^{15}\text{N}_{\text{bulk}}$ values in moss samples. The FAA and bulk data were compared to determine whether FAAs can be effectively used to assess N deposition. The aims were (1) to assess the relationship between FAA N concentrations and atmospheric N deposition, (2) to determine how to using highly variable $\delta^{15}\text{N}_{\text{FAA}}$ values indicate atmospheric N sources, and (3) to determine which specific $\delta^{15}\text{N}_{\text{FAA}}$ value best reflects N sources to the atmosphere.

Results

Bulk N concentrations and $\delta^{15}\text{N}_{\text{bulk}}$. The bulk N concentrations in the moss samples were 1.1%–3.0%, and the mean was $1.9\% \pm 0.6\%$, as shown in Fig. 1a. The mean bulk N concentrations in moss from the seven sites in Nanchang City were decreased in the order urban centre ($2.7\% \pm 0.4\%$), landfill ($2.5\% \pm 0.3\%$), airport ($1.9\% \pm 0.3\%$), zoo ($1.4\% \pm 0.2\%$) and suburbs ($1.2\% \pm 0.1\%$). The mean bulk N concentrations were significantly higher in Urban than those in Suburbs ($p < 0.05$).

As shown in Fig. 2, most moss samples had negative mean $\delta^{15}\text{N}_{\text{bulk}}$ values. The mean $\delta^{15}\text{N}_{\text{bulk}}$ was $-4.0\% \pm 2.9\%$ and the interquartile range was -5.7% to -1.3% .

FAA concentrations. The Ala, Arg, Asn, Asp, Gaba, Gln, Glu, Gly, His, Ile, Leu, Lys, Met, Phe, Pro, Ser, Thr, Trp, Tyr, and Val concentrations in the moss samples are shown in Table S1. The concentrations of TFAA ($943.9\text{--}11100.5\ \mu\text{g g}^{-1}$; Fig. 1b), Gln (not detected to $303.5\ \mu\text{g g}^{-1}$; Fig. 1c), Asn ($6.18\text{--}750.9\ \mu\text{g g}^{-1}$; Fig. 1d), Glu ($49.7\text{--}2159.9\ \mu\text{g g}^{-1}$; Fig. 1e), and Arg ($114.0\text{--}2117.3\ \mu\text{g g}^{-1}$; Fig. 1f) in the samples from the different sites varied in similar ways to the bulk N concentrations (Fig. 1a). The FAA concentrations were significantly higher in the samples from the urban centre than from the suburbs ($p < 0.05$).

The N concentrations of Arg, Asn, Asp, Gln, Glu, Ser, and TFAA strongly positively correlated with atmospheric N deposition ($P < 0.05$) (Fig. 3). The equations for the relationships between the Arg, Asn, Asp, Gln, Glu, Ser, and TFAA concentrations and atmospheric N deposition are shown in Table S2.

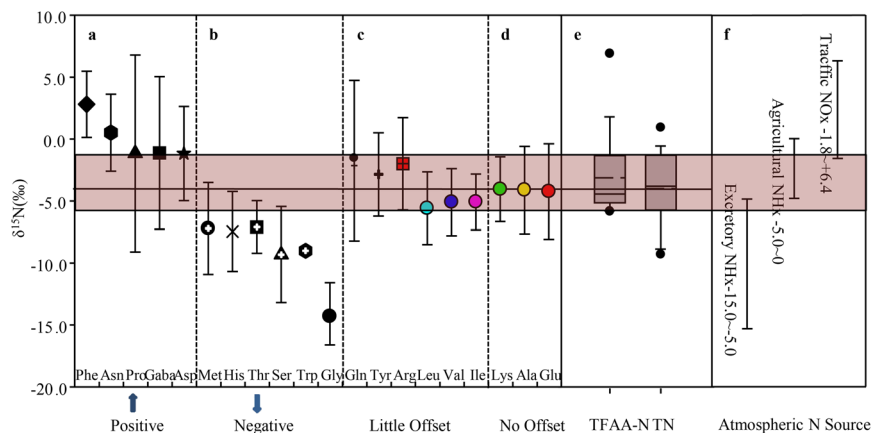


Figure 2. Moss $\delta^{15}\text{N}$ of individual FAAs in NanChang city. The vertical lines represent standard deviations. Moss $\delta^{15}\text{N}_{\text{TFAA}}$ and $\delta^{15}\text{N}_{\text{TN}}$ were showed in box plot. The box encloses 50% of the data, the whiskers 90% of the data, the solid lines is the median, the dashed line is the mean, solid circles are outliers. The $\delta^{15}\text{N}$ ranges of the potential N sources are also included in the figure. The date of NH_x $\delta^{15}\text{N}$ values from excretory wastes is cited from Freyer⁵⁹; Heaton⁶⁰ and Moore⁶¹. NH_x $\delta^{15}\text{N}$ values from agricultural source is referenced from Xiao *et al.*⁵⁸. The $\delta^{15}\text{N}$ value of NO_x is cited from Freyer⁵⁹ and Saurer *et al.*⁶⁷.

$\delta^{15}\text{N}$ values for individual FAAs ($\delta^{15}\text{N}_{\text{FAA}}$). The $\delta^{15}\text{N}_{\text{FAA}}$ values for the moss samples varied widely, from -19.3‰ to $+16.1\text{‰}$ (Fig. 4). The FAAs were placed in four groups depending on how the $\delta^{15}\text{N}_{\text{FAA}}$ compared with the $\delta^{15}\text{N}_{\text{bulk}}$ interquartile range. As shown in Fig. 2, the mean $\delta^{15}\text{N}$ values for Ala (-4.1‰), Glu (-4.2‰), and Lys (-4.0‰) (group d) were close to the mean $\delta^{15}\text{N}_{\text{bulk}}$ (-4.0‰). The mean $\delta^{15}\text{N}$ values for Arg (-2.0‰), Gln (-1.7‰), Ile (-5.1‰), Leu (-5.6‰), Tyr (-2.9‰), and Val (-5.1‰) (group c) were between the $\delta^{15}\text{N}_{\text{bulk}}$ interquartiles (-5.7‰ and -1.3‰). The $\delta^{15}\text{N}$ values for Gly (-14.3‰), His (-7.5‰), Met (-7.2‰), Ser (-9.3‰), Thr (-7.1‰), and Trp (-9.0‰) (group b) were below the lower $\delta^{15}\text{N}_{\text{bulk}}$ quartile. The $\delta^{15}\text{N}$ values for Asn ($+0.5\text{‰}$), Asp (-1.2‰), Gaba (-1.1‰), Phe ($+2.8\text{‰}$), and Pro (-1.2‰) (group a) were higher than the upper $\delta^{15}\text{N}_{\text{bulk}}$ quartile.

Concentration-weighted mean $\delta^{15}\text{N}$ values for the TFAA ($\delta^{15}\text{N}_{\text{TFAA}}$). The FAA $\delta^{15}\text{N}$ values varied widely, there being a 35‰ difference between the highest and lowest, as shown in Fig. 4. The $\delta^{15}\text{N}_{\text{TFAA}}$ values were calculated using the isotope mass-balance equation

$$\delta^{15}\text{N}_{\text{TFAA}} = \frac{\sum \delta^{15}\text{N}_i \cdot \text{C}_i \cdot \text{n}_i}{\sum \text{C}_i \cdot \text{n}_i}, \quad (1)$$

where $\delta^{15}\text{N}_i$ is the $\delta^{15}\text{N}$ value for FAA i , C_i is the molar concentration of FAA i , and n_i is the number of N atoms in FAA i . The mean $\delta^{15}\text{N}_{\text{TFAA}}$ was $-3.1\text{‰} \pm 3.2\text{‰}$ (Fig. 4) and the interquartile range (-5.2‰ to -1.3‰) was similar to the $\delta^{15}\text{N}_{\text{bulk}}$ interquartile range (Fig. 2).

Fractionation of individual FAA normalized to $\delta^{15}\text{N}_{\text{bulk}}$. The method used to calculate positive and negative fractionation of individual FAA normalized to $\delta^{15}\text{N}_{\text{bulk}}$ is shown in Fig. S1. The FAAs were divided into three groups depending on the $\delta^{15}\text{N}_{\text{FAA}}$ values relative to the mean $\delta^{15}\text{N}_{\text{bulk}}$ (-4.0‰). In group δ_1 , the FAA $\delta^{15}\text{N}$ values were $>0\text{‰}$. In group δ_2 , the FAA $\delta^{15}\text{N}$ values were $>-4.0\text{‰}$ but $<0\text{‰}$. In group δ_3 , the FAA $\delta^{15}\text{N}$ values were $<-4.0\text{‰}$. N isotope fractionation relative to $\delta^{15}\text{N}_{\text{bulk}}$ for all three groups was calculated using equation 2.

$$\Delta^{15}\text{N} = \frac{\sum (\delta^{15}\text{N}_i + 4) \text{C}_i}{\sum \text{C}_i} \quad (2)$$

The total positive fractionation relative to $\delta^{15}\text{N}_{\text{bulk}}$ ($\Delta^{15}\text{N}_{\text{positive}} + 3.4\text{‰}$) was equal to the total negative fractionation relative to $\delta^{15}\text{N}_{\text{bulk}}$ ($\Delta^{15}\text{N}_{\text{negative}} - 3.6\text{‰}$) (Fig. 5).

Spearman correlations between $\delta^{15}\text{N}_{\text{FAA}}$, $\delta^{15}\text{N}_{\text{bulk}}$, and $\delta^{15}\text{N}_{\text{TFAA}}$. Linear regression analyses indicated that the $\delta^{15}\text{N}_{\text{bulk}}$ values significantly correlated with the $\delta^{15}\text{N}_{\text{TFAA}}$ values and the $\delta^{15}\text{N}$ values for Ala, Gaba, His, Ile, Leu, Lys, and Ser ($p < 0.05$). $\delta^{15}\text{N}_{\text{TFAA}}$ significantly correlated with the $\delta^{15}\text{N}$ values for most of the FAAs (Ala, Arg, Asn, Asp, Gaba, Glu, Gly, His, Ile, Leu, Lys, Pro, Ser, and Val) ($p < 0.05$). $\delta^{15}\text{N}_{\text{Glu}}$ correlated with the $\delta^{15}\text{N}$ values for almost all of the FAAs except for Gaba, Gln, Ile, Met, Phe, Thr, Trp, and Tyr ($p < 0.05$) (Table S3).

Discussion

Strong relationships between individual FAA (mainly Arg, Asn, Asp, Glu, Gln, Ser, and TFAA) and atmospheric N deposition have been found in various moss species (Table S2)^{19,44–46}. In our study, the concentrations of TFAA and some FAAs also varied spatially in similar ways to the bulk N concentration (Fig. 1) and positively correlated with atmospheric N deposition (Fig. 3). The abilities of FAAs in moss to respond to N inputs are related to

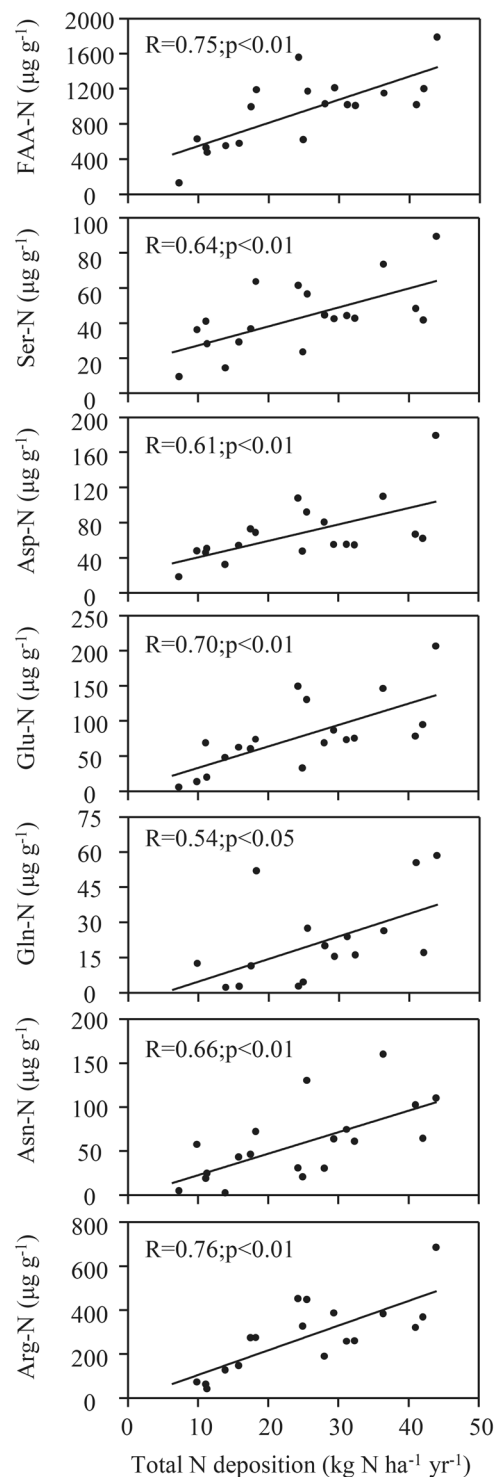


Figure 3. Relationships between concentrations of individual FAA (expressed as N concentrations) in moss and estimated total atmospheric N deposition. $C_{\text{FAA-N}}$ calculated by: $C_{\text{FAA-N}} = C_{\text{FAA}} \cdot n \cdot 14$. C_{FAA} is the molar concentration of each amino acid; n is the nitrogen atoms contained in each AA; 14 is the relative molecular mass of nitrogen atom. Total atmospheric N deposition (x) at each sampling sites was estimated using the linear correlation equation ($y = 0.052x + 0.73$, $R^2 = 0.70$, $P < 0.001$; Xiao *et al.*⁵⁸) between atmospheric N deposition (x) values and the corresponding moss TN concentrations (y) from the Yangtze River drainage basin.

the chemical and physiological characteristics of the FAAs. When high N deposition occurs, the Gln, Arg, and Asn concentrations increased because these FAAs have low C:N ratios⁴⁰. Moreover, larger changes in free amino acid concentrations responded to increased atmospheric N additions than total N has been observed in various

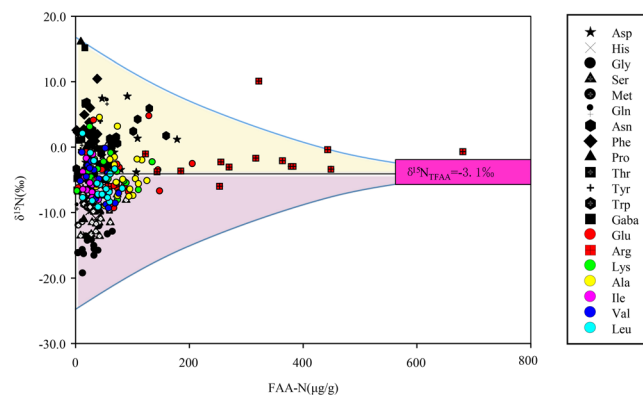


Figure 4. The $\delta^{15}\text{N}$ values of free amino acids (‰) vs. the concentrations of free amino acids (expressed as N concentrations, $\mu\text{g/g}$) in mosses. $\delta^{15}\text{N}_{\text{TFAA}} = -3.1\text{‰}$ is concentration-weighted average nitrogen isotope of free amino acids calculated by Rayleigh equilibrium equation.

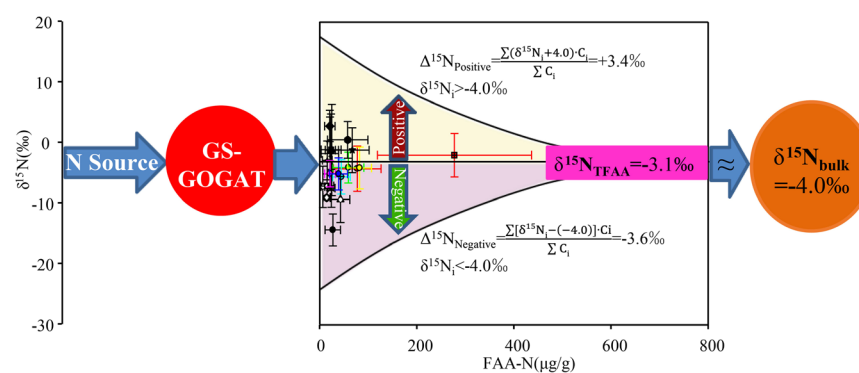


Figure 5. Relationship between $\delta^{15}\text{N}_{\text{source}}$, $\delta^{15}\text{N}_{\text{TFAA}}$ and $\delta^{15}\text{N}_{\text{bulkN}}$. Total ^{15}N -enrichment for individual FAA and total ^{15}N -depletion vs. $\delta^{15}\text{N}_{\text{bulk}}$ (-4.0‰) are also showed.

studies. Baxter, *et al.*⁴⁷ found dramatic transient increases in the concentrations of Arg (by a factor of 19), Asn (by a factor of 4), and Gln (by a factor of 3) in moss exposed to 0.1 mM NH_4^+ for 20 d. Huhn and Schulz¹⁸ found that Arg accumulated much more strongly in Rōsa (high N concentrations) than in Neuglobsow (low N deposition), the Arg concentration being 150 times higher in moss from Rōsa than in moss from Neuglobsow. Similarly, in this study, we found that Glu (7-fold), Arg (9-fold), Gln (12-fold) and Asn (4-fold) increased large proportion than total nitrogen (2-fold). The synthesis of N-rich FAAs minimizes carbon use for storing N and avoids toxic concentrations of NH_4^+ accumulating in plant tissues^{48–51}. Additional metabolic features have been found to be responsible for increases in the concentrations of these FAAs in high nitrogen deposition. For example, Arg is more soluble than other FAAs^{19,25,52}, Glu plays a central role in N uptake¹⁸, Gln increases the photosynthetic capacities of plants^{44,53}, and Ser is involved in the photorespiratory N cycle⁴⁷. It is therefore possible that the concentrations, expressed as N concentrations, of some FAAs (Arg, Asn, Asp, Gln, Glu, Ser, and TFAA) in moss could indicate current atmospheric N deposition.

The development of isotopic analysis methods has led to $\delta^{15}\text{N}$ values for amino acids being regarded as important tracers of the sources of and transformation processes affecting N-containing compounds in plant tissues^{41,42,54}. However, the $\delta^{15}\text{N}$ values for the 20 FAAs mentioned above were very different, suggesting marked N isotope fractionation occurred during the uptake, translocation, biosynthetic, and metabolic pathways^{38,55,56}. Gauthier, *et al.*³⁸ found that isotope fractionation between nitrate and Glu gave a $\delta^{15}\text{N}$ value of 15.8‰ and that isotope fractionation associated with Asn synthesis from Asp gave $\delta^{15}\text{N}$ values up to 36‰. In our study, the FAA $\delta^{15}\text{N}$ values for moss covered a wide range, from -19.3‰ to $+16.1\text{‰}$ (Fig. 4). Little or no N isotope fractionation has been assumed to occur during N uptake and translocation in mosses³⁴, so the large variations in the FAA $\delta^{15}\text{N}$ values could mainly have been caused by FAA metabolism pathways.

Numerous atmospheric N compounds are directly taken up by moss, and little isotopic fractionation is associated with N assimilation. It has previously been found that $\delta^{15}\text{N}_{\text{bulk}}$ values for mosses are good indicators of atmospheric N sources^{30,36,57,58}. The mean $\delta^{15}\text{N}_{\text{bulk}}$ value for the moss samples from Nanchang City was $-4.0\text{‰} \pm 2.9\text{‰}$ (range -9.3‰ to $+0.9\text{‰}$). According to $\delta^{15}\text{N}$ inventories for potential N sources^{59–61}, atmospheric N may be deposited in Nanchang mainly as NH_y (negative $\delta^{15}\text{N}$ values, group f in Fig. 2) originally emitted in animal excreta (-15.0‰ to -5.0‰)^{59–61} and during agricultural processes (-5‰ to 0‰)⁵⁸. This conclusion was drawn because of the negative $\delta^{15}\text{N}$ values. This result agreed with the results of a previous study of urban, rural, and forested sites in South China¹¹. However, most of the $\delta^{15}\text{N}_{\text{TFAA}}$ values were very different from the $\delta^{15}\text{N}_{\text{bulk}}$ values and the

$\delta^{15}\text{N}_{\text{FAA}}$ range was much wider (35‰) than the $\delta^{15}\text{N}_{\text{bulk}}$ range (10‰). It would therefore have been somewhat difficult for the $\delta^{15}\text{N}_{\text{FAA}}$ values to indicate the N sources because of isotopic fractionation caused by metabolism, as discussed above.

It has been shown in numerous studies that FAA $\delta^{15}\text{N}$ values are related to fractionation in the FAA metabolic pathways^{38,39,43,62–64}. In this study the AA- $\delta^{15}\text{N}$ pattern for free amino acid contrasted to the average value of $\delta^{15}\text{N}_{\text{TFAA}}$, to discuss the fractionation with free amino acids metabolic pathways. Compared to the average value of $\delta^{15}\text{N}_{\text{TFAA}}$, Gln, Phe, Tyr, Asn and Asp have higher $\delta^{15}\text{N}$ value vs. $\delta^{15}\text{N}_{\text{TFAA}}$ (Fig. 2). Relative enrichment of ^{15}N in Phe has been found to be related to kinetic isotope effects associated with the Phenylalanine ammonia-lyase catalyses Phe deamination, leaving the residual Phe relatively enriched in ^{15}N ^{39,62,65}. Tyr is catalyzed by tyrosine ammonia-lyase to 4-hydroxycinnamate, which associated with marked ^{15}N enrichment in Tyr. The $\delta^{15}\text{N}$ value of Pro is positive than the value of $\delta^{15}\text{N}_{\text{TFAA}}$, it could be explained by the kinetic isotope effect involved in the catabolism of Pro is greater than that its biosynthesis procedure or the biosynthesis of Pro is an thermodynamic procedure⁵⁴. Relative ^{15}N -enrichment in Asp is caused by the transfer of the amino group from Glu to oxaloacetate to form Asp, involving the formation of a protonated Schiff base, favouring ^{15}N for Asp production⁵⁶. Styring, *et al.*⁵⁴ attributed ^{15}N enrichment in Asn in cereal grains to Asn acting as a transport metabolite. The amino group of Asn is incorporated into other amino acids through transamination with α -keto acids, involving kinetic isotope fractionation discriminating against ^{15}N . On the other hand, Gly and Ser have depleted $\delta^{15}\text{N}$ values vs. $\delta^{15}\text{N}_{\text{TFAA}}$ (Fig. 2). Gly and Ser involve the photorespiratory cycle in the plants. ^{15}N -depletion in Gly and Ser was possibly caused by ^{15}N -depletion reaction during photorespiration related to Gly and Ser formation, e.g., isotope effect associated with transamination from Glu to produce Gly and discrimination against ^{15}N associated with the reaction that converts Gly to Ser^{38,63,66}.

Obviously using $\delta^{15}\text{N}_{\text{FAA}}$ values to indicate atmospheric N sources could therefore be affected by isotopic fractionation during FAA metabolic reactions in moss, as discussed above. The $\delta^{15}\text{N}$ values for some FAAs may not reliably reflect atmospheric N sources. For example, using ^{15}N -enriched FAAs (e.g., Phe, $\delta^{15}\text{N}_{\text{Phe}} 2.8\text{‰} \pm 2.7\text{‰}$) to identify the main sources of atmospheric N deposition would incorrectly identify the source of N deposition in Nanchang City as being traffic-derived NO_2 ($\delta^{15}\text{N} +1.3\text{‰}$ to $+6.4\text{‰}$)⁶⁷, whereas using FAAs with more negative $\delta^{15}\text{N}$ values (e.g., Gly, $\delta^{15}\text{N}_{\text{Gly}} -14.3\text{‰} \pm 2.7\text{‰}$) would indicate the sources being animal excreta ($\delta^{15}\text{N} -15.2\text{‰}$ to -8.9‰) and sewage ($\delta^{15}\text{N} -15\text{‰}$ to -4‰)^{59,60}. We attempted to use $\delta^{15}\text{N}_{\text{TFAA}}$ as an indicator to solve this. As shown in Fig. 5, the sum of the positive differences between individual $\delta^{15}\text{N}_{\text{FAA}}$ values and $\delta^{15}\text{N}_{\text{bulk}}$ ($\Delta^{15}\text{N}_{\text{positive}} +3.4\text{‰}$) was equal to the sum of the negative differences between individual $\delta^{15}\text{N}_{\text{FAA}}$ values and $\delta^{15}\text{N}_{\text{bulk}}$ ($\Delta^{15}\text{N}_{\text{negative}} -3.6\text{‰}$), implying that the TFAAs were isotopically equilibrated during FAA metabolism in the moss. The mean $\delta^{15}\text{N}_{\text{TFAA}}$ ($-3.1\text{‰} \pm 3.2\text{‰}$) was close to $\delta^{15}\text{N}_{\text{bulk}}$ ($-4.0\text{‰} \pm 2.9\text{‰}$), and the $\delta^{15}\text{N}_{\text{TFAA}}$ interquartile range (-5.2‰ to -1.3‰) was similar to the $\delta^{15}\text{N}_{\text{bulk}}$ interquartile range (-5.7‰ to -1.3‰) (group e in Fig. 2), that is, $\delta^{15}\text{N}_{\text{TFAA}} \approx \delta^{15}\text{N}_{\text{bulk}} \approx \delta^{15}\text{N}_{\text{Source}}$. The Pearson correlations indicated that $\delta^{15}\text{N}_{\text{TFAA}}$ significantly correlated with $\delta^{15}\text{N}_{\text{bulk}}$ (Table S3). We therefore concluded that little isotopic fractionation occurs between TFAA and bulk N, meaning $\delta^{15}\text{N}_{\text{TFAA}}$ for moss can be used to indicate atmospheric N sources.

Most $\delta^{15}\text{N}_{\text{FAA}}$ values have not been compared with $\delta^{15}\text{N}_{\text{bulk}}$ values, so it is not clear which $\delta^{15}\text{N}_{\text{FAA}}$ values in moss best indicate N source signatures. Only similar trends in $\delta^{15}\text{N}_{\text{FAA}}$ and $\delta^{15}\text{N}_{\text{sources}}$ have been reported in previous publications. Chikaraishi, *et al.*⁶⁸ found more ^{15}N -depleted FAAs in moss from more industrial areas than in moss from more agricultural areas. Xu and Xiao⁴² found that Ala, Arg, Asp, Glu, His, Ile, Lys, Pro, Ser, and TFAA were more ^{15}N -depleted in needles from sites far from highways than in needles from sites near highways, suggesting that atmospheric $\text{NH}_x\text{-N}$ from soil emissions affect $\delta^{15}\text{N}_{\text{FAA}}$ values more for needles far from highways than for needles near highways. However, $\delta^{15}\text{N}$ values for most FAAs used as indicators were quite different from $\delta^{15}\text{N}$ values for environmental N sources in a study by Xu and Xiao⁴². They found $\delta^{15}\text{N}_{\text{Gln}}$ values $< -8\text{‰}$ for new needles at 800 from the highway. These $\delta^{15}\text{N}_{\text{Gln}}$ values may possibly indicating a more ^{15}N -depleted N source such as animal excreta ($\delta^{15}\text{N} -15\text{‰}$ to -5‰) rather than $\text{NH}_x\text{-N}$ from soil ($\delta^{15}\text{N} -5.8\text{‰}$ to -3.3‰)^{59,60}. If using $\delta^{15}\text{N}$ of specific free amino acid with large fractionation in their metabolism to indicate atmospheric N sources, a misleading conclusion would be obtained. It was unexpected that only a portion of the free amino acid $\delta^{15}\text{N}$ values can hold N source signatures. We compared the $\delta^{15}\text{N}_{\text{FAA}}$ to $\delta^{15}\text{N}_{\text{bulk}}$ values for the 20 FAAs to identify which $\delta^{15}\text{N}$ values best indicated atmospheric N sources. The mean $\delta^{15}\text{N}_{\text{Glu}}$, $\delta^{15}\text{N}_{\text{Ala}}$, and $\delta^{15}\text{N}_{\text{Lys}}$ values were very similar to the $\delta^{15}\text{N}_{\text{bulk}}$ values (Fig. 2). This may have been because no or little isotope fractionation was associated with the metabolic pathways of these FAAs. The main roles of Glu in FAA metabolism in plant tissues are to provide an amino group for the biosynthesis of other amino acids and to receive amino groups from the catabolism of other FAAs, which were confirmed in needles, cereal, pulse, algae and wheat tissues^{41,54,69–71}. Our results confirmed this from the N isotope viewpoint in that $\delta^{15}\text{N}_{\text{Glu}}$ significantly correlated with the $\delta^{15}\text{N}$ values for most of the FAAs and with $\delta^{15}\text{N}_{\text{TFAA}}$ ($p < 0.05$) (Table S3) and in that $\delta^{15}\text{N}_{\text{Glu}}$ (-4.0‰) was similar to $\delta^{15}\text{N}_{\text{TFAA}}$ (-3.1‰) (Fig. 2). We also found that the measured $\delta^{15}\text{N}_{\text{Ala}}$ value was similar to the measured $\delta^{15}\text{N}_{\text{Glu}}$, which would have been because kinetic isotope effects on the biosynthesis of Ala from pyruvate and Glu are weak^{39,43,72}. Numerous previously also found that biosynthesizing branched-chain from pyruvate and Glu associated by low kinetic isotope effect^{39,72}. Lys displayed no significant offset to the average value of $\delta^{15}\text{N}_{\text{TFAA}}$. Gauthier, *et al.*³⁸ found that, in plants, Lys acquires N derived from Glu, so $\delta^{15}\text{N}_{\text{Lys}}$ will reflect $\delta^{15}\text{N}_{\text{Glu}}$. This could help explain why $\delta^{15}\text{N}_{\text{Lys}}$ was equal to the mean $\delta^{15}\text{N}_{\text{bulk}}$ in our study. The $\delta^{15}\text{N}_{\text{bulk}}$ value for moss reliably indicates atmospheric N sources, so we concluded that free Ala, Glu, and Lys (which are little affected by kinetic isotope effects during metabolism) may preserve information on atmospheric N sources.

Conclusions

The concentrations (expressed as N) of some FAAs (e.g., Arg, Asn, Asp, Gln, Glu, Ser, and TFAA) in moss were positively correlated with total atmospheric N deposition, indicating that the concentrations of those FAAs in moss could indicate atmospheric N deposition with a good degree of sensitivity.



Figure 6. The locations of moss sampling sites in Nanchang city. The locational map was modified from Google Earth 7.1.5.1557 (<http://earth.google.com>).

We first used the FAA N isotope compositions to determine whether FAA metabolism in moss could reflect atmospheric N sources. The FAA $\delta^{15}\text{N}$ values for the moss varied widely, probably mainly caused by the FAA metabolic pathways in the moss. However, total FAAs are at isotopic equilibrium during FAA metabolism and that the moss $\delta^{15}\text{N}_{\text{TFAA}}$ value could reliably indicate atmospheric N sources. We also found that the $\delta^{15}\text{N}$ values of some FAAs (such as Ala, Glu, and Lys) preserve information on atmospheric N sources as well as $\delta^{15}\text{N}_{\text{bulk}}$ preserves this information because little isotope fractionation occurs in the metabolic pathways of these FAAs.

Future work should include an investigation of FAA $\delta^{15}\text{N}$ variability in vascular plants under different N deposition conditions to allow the kinetic isotope effects of N transport in different plant organs to be investigated.

Materials and Methods

Sample collection and treatment. *Haplocladium microphyllum* (Hedw.) moss samples were collected from urban, suburban, landfill, and airport sites in Nanchang City (South China) in July 2017. The sampling locations are shown in Fig. 6. Only green, healthy moss was sampled. The sampling sites were chosen based on the results of previous studies^{73,74}. Each moss sample was collected from natural rocks in an open field away from overhanging vegetation or tree canopy. Sites were excluded if they could have been affected by point sources of N, such as soil, surface water, or domestic animals. Each sample was collected at least 500 m from any main road and at least 100 m from any other road or a house. Two–four sampling sites were selected in each plot, and 5–10 subsamples were collected at each site, then the subsamples were mixed (to ensure each sample was representative).

Each moss sample was immediately placed in a chilled insulated box. Adsorbed pollutants were removed by gently rinsing each sample with deionized water several times. Half of each washed sample was dried at 80 °C for 1 d, and the other half was freeze-dried. Each dry sample was ground to a fine powder and stored at –80 °C until analysis⁶⁸.

Bulk N and $\delta^{15}\text{N}_{\text{bulk}}$ analyses. The bulk N concentration (expressed in % on a dry weight basis) and $\delta^{15}\text{N}_{\text{bulk}}$ were determined simultaneously using a Flash EA 2000 elemental analyser (Thermo Scientific, Bremen, Germany) connected to a Thermo MAT253 plus isotope ratio mass spectrometer (Thermo Scientific, Bremen, Germany). The N concentration analytical precision was better than 0.1%. The $\delta^{15}\text{N}$ method was calibrated by analysing caffeine (IAEA-600, $\delta^{15}\text{N} = +1.0\text{‰}$), ammonium sulfate (USGS25, $\delta^{15}\text{N} = -30.4\text{‰}$), and L-glutamic acid (USGS 41a, $\delta^{15}\text{N} = +47.6\text{‰}$) standards with each set of samples. The $\delta^{15}\text{N}$ analytical precision (standard deviation; $n = 3$) was better than $\pm 0.05\text{‰}$. The isotope ratios were expressed in per mil (‰) relative to atmospheric N_2 . Each N concentration and $\delta^{15}\text{N}$ value reported is the mean of at least three measurements.

FAA extraction, purification, and derivatization. The FAAs were extracted using a method described by Gauthier, *et al.*³⁸. Briefly, 0.2–1 g of moss powder was suspended in distilled water, centrifuged for 5 min at 10000 g and 5 °C, then the supernatant was transferred to another centrifuge tube. The sample was extracted again, and the supernatants were mixed and heated to 100 °C for 5 min to precipitate proteins. The extract was then centrifuged for 5 min at 10000 g and 5 °C, then 100 μL of 1 nmol μL^{-1} α -aminobutyric acid was added to act as an internal reference ($\delta^{15}\text{N} = -8.17\text{‰} \pm 0.03\text{‰}$). The extract was then freeze-dried and resuspended in 1 mL of 0.1 mol L^{-1} HCl. The extract was then passed through a cation exchange column (Dowex 50WX8 H^+ , 200–400 mesh; Sigma-Aldrich, St Louis, MO, USA), and the amino-acid-enriched fraction was stored at –80 °C until analysis.

tert-Butyldimethylsilyl (tBDMS) derivatives of the amino acids were prepared following methods described by Molero, *et al.*⁵⁵ and Zhang, *et al.*⁷⁵. Approximately 150 µg anhydrous Na₂SO₄, 50 µL pyridine, and 50 µL N-methyl-N-(*tert*-butyldimethylsilyl) trifluoroacetamide were added in sequence to freeze dried amino acids, then the mixture was incubated at 70 °C for 1 h.

Determining amino acid concentrations and δ¹⁵N values. Amino acid concentrations and compound-specific structural and δ¹⁵N values were determined by analysing the *tert*-butyldimethylsilyl derivatives by gas chromatography (GC)/MS/IRMS. The GC/MS/IRMS instrument had a Trace GC instrument (Thermo Fisher Scientific), from which ~10% of the outflow entered a ISQ QD single quadrupole MS instrument (Thermo Fisher Scientific) to allow concentration and structural information to be acquired for each eluting peak. The remaining ~90% of the outflow entered a Thermo GC-isolink, in which the eluted compounds were oxidized and reduced to form CO₂ and N₂. The gases then entered a ConFlo IV interface (Thermo Fisher Scientific) and then a Delta V IRMS instrument (Thermo Fisher Scientific) to allow δ¹⁵N isotope data to be acquired.

The instrument conditions are described below. The injection volume was 0.2–1.0 µL, and splitless mode was used. The autosampler injector temperature was 270 °C. Separation was achieved using a DB-5 column (30 m long, 0.25 mm i.d., 0.25 µm film thickness; Agilent Technologies, Santa Clara, CA, USA). The carrier gas was helium, and the flow rate was 1.0 mL/min. The system was back-flushed with helium for 900 s during each analysis. The GC oven temperature started at 90 °C (held for 1 min), then increased at 12 °C min⁻¹ to 150 °C (held for 5 min), increased at 3 °C min⁻¹ to 220 °C, then increased at 12 °C min⁻¹ to 285 °C (held for 7.5 min). The combustion reactor was held at 1,000 °C.

The linearity of the GC/MS method was assessed by evaporating, derivatizing, and analysing a series of standards containing 20 amino acids at concentrations of 0.04–1 mM. Each standard contained alanine (Ala), γ-aminobutyric acid (Gaba), arginine (Arg), asparagine (Asn), aspartate (Asp), glutamine (Gln), glutamate (Glu), glycine (Gly), histidine (His), isoleucine (Ile), leucine (Leu), lysine (Lys), methionine (Met), phenylalanine (Phe), proline (Pro), serine (Ser), threonine (Thr), tryptophan (Trp), tyrosine (Tyr), and valine (Val). The concentration of each amino acid was determined from the GC-MS signal using the relevant calibration curve produced from the standard amino acid mix data and corrected for the α-aminobutyric acid recovery. The R² values for the calibration curves were 0.9909–0.9969, indicating that the method was accurate.

A derivatized mixture of 20 amino acid standards and several single amino acid standards (Ala Gly3, Gly4, Phe, USGS40, USGS41a, and Val) with known δ¹⁵N values (−26.35 to +47.55‰) was prepared to allow instrumental performance to be monitored and drift to be corrected. The amino acids were successfully converted into TBDMS derivatives and could be completely resolved by GC-C-IRMS (Fig. S2). The results are shown in Table S4. The α-aminobutyric acid (internal standard) δ¹⁵N value for each sample was used to confirm that the isotope measurements were reproducible. The 20 amino acid standard mixture was analysed after every three samples during a GC/MS/IRMS run to assess the isotope measurement reproducibility and normalize the δ¹⁵N values of the amino acids in the samples⁴². The amount of sample analysed by GC/MS/IRMS needed to be considered. Standard mixture containing the 20 amino acids each at an equivalent of 0.8 nmol (equivalent to FAA concentration of 9–20 µg g⁻¹ in moss) was analysed to allow the δ¹⁵N values of low concentrations of amino acids to be determined. The FAA concentrations expressed as N concentrations in our samples were higher than these concentrations. The δ¹⁵N measurement precisions (n = 9) for the derivatized amino acid standard mixtures were 0.5‰–1.4‰ (Table S4). The δ¹⁵N values for the underivatized amino acids measured by elemental analysis/IRMS correlated with the δ¹⁵N values for the derivatized amino acids measured by GC/MS/IRMS (R² = 0.997, P < 0.001). The differences between the empirically corrected δ¹⁵N values measured by elemental analysis/IRMS and GC/MS/IRMS were 0.1‰–1.3‰ (Table S4). Each value reported here is the mean of at least three δ¹⁵N determinations.

Statistical analysis. Statistical analyses were performed using SPSS 16.0 software (IBM, Armonk, NY, USA). The statistical significances of differences in the FAA contents of samples from different sites were tested using the one-way analysis of variance method and Tukey-HSD tests, and differences were considered significant at P < 0.05. Correlations between δ¹⁵N_{FAA}, δ¹⁵N_{TFAA}, and δ¹⁵N_{bulk} were assessed using Pearson correlation coefficients (r). Linear regressions were used to identify correlations between the FAA concentrations and estimated atmospheric N deposition. Most graphs were drawn using SigmaPlot 10.0 software (Systat Software, San Jose, CA, USA).

Data Availability

All data generated or analyzed during this study are included in this published article and its Supplementary Information file.

References

- Galloway, J. N. *et al.* Transformation of the Nitrogen Cycle: Recent Trends, Questions, and Potential Solutions. *Science* **320**, 889–892 (2008).
- Galloway, J. N. *et al.* Nitrogen cycles: past, present, and future. *Biogeochemistry* **70**, 153–226 (2004).
- Vitousek, P. M. *et al.* Technical Report: Human Alteration of the Global Nitrogen Cycle: Sources and Consequences. *Ecological Applications* **7**, 737–750 (1997).
- Bobbink, R. *et al.* Global assessment of nitrogen deposition effects on terrestrial plant diversity: a synthesis. *Ecological Applications: A Publication of the Ecological Society of America* **20**, 30 (2010).
- Clark, C. M. & Tilman, D. Loss of plant species after chronic low-level nitrogen deposition to prairie grasslands. *Nature* **451**, 712–715 (2008).
- Matson, P., Lohse, K. A. & Hall, S. J. The Globalization of Nitrogen Deposition: Consequences for Terrestrial Ecosystems. *Ambio* **31**, 113–119 (2002).

7. Richter, A., Burrows, J. P., Nüss, H., Granier, C. & Niemeier, U. Increase in tropospheric nitrogen dioxide over China observed from space. *Nature* **437**, 129–132 (2005).
8. Harmens, H. *et al.* Nitrogen concentrations in mosses indicate the spatial distribution of atmospheric nitrogen deposition in Europe. *Environmental Pollution* **159**, 2852–2860 (2011).
9. Harmens, H. *et al.* Relationship between site-specific nitrogen concentrations in mosses and measured wet bulk atmospheric nitrogen deposition across Europe. *Environmental Pollution* **194**, 50–59 (2014).
10. Koranda, M., Kerschbaum, S., Wanek, W., Zechmeister, H. & Richter, A. Physiological Responses of Bryophytes *Thuidium tamariscinum* and *Hylocomium splendens* to Increased Nitrogen Deposition Koranda *et al.* — Physiological Responses of Bryophytes. *Ann Bot* **99**, 161–169 (2007).
11. Xiao, H. Y., Tang, C. G., Xiao, H. W., Liu, X. Y. & Liu, C. Q. Stable sulphur and nitrogen isotopes of the moss *Haplocladium microphyllum* at urban, rural and forested sites. *Atmospheric Environment* **44**, 4312–4317 (2010).
12. Armitage, H. F. *et al.* Nitrogen deposition enhances moss growth, but leads to an overall decline in habitat condition of mountain moss-sedge heath. *Global Change Biology* **18**, 290–300 (2012).
13. Bragazza, L. *et al.* Nitrogen concentration and delta¹⁵N signature of ombrotrophic Sphagnum mosses at different N deposition levels in Europe. *Global Change Biology* **11**, 106–114 (2005).
14. Limpens, J. *et al.* Glasshouse vs field experiments: do they yield ecologically similar results for assessing N impacts on peat mosses? *New Phytologist* **195**, 408–418 (2012).
15. Liu, X. Y., Xiao, H. Y., Liu, C. Q., Li, Y. Y. & Xiao, H. W. Tissue N content and 15 N natural abundance in epilithic mosses for indicating atmospheric N deposition in the Guiyang area, SW China. *Applied Geochemistry* **23**, 2708–2715 (2008).
16. Pitcairn, C. *et al.* Diagnostic indicators of elevated nitrogen deposition. *Environmental Pollution* **144**, 941–950 (2006).
17. Solga, A., Burkhardt, J., Zechmeister, H. G. & Frahm, J. P. Nitrogen content, 15N natural abundance and biomass of the two pleurocarpous mosses *Pleurozium schreberi* (Brid.) Mitt. and *Scleropodium purum* (Hedw.) Limpr. in relation to atmospheric nitrogen deposition. *Environmental Pollution* **134**, 465–473 (2005).
18. Huhn, G. & Schulz, H. Contents of free amino acids in Scots pine needles from field sites with different levels of nitrogen deposition. *New Phytologist* **134**, 95–101 (1996).
19. Nordin, A., Nasholm, T. & Ericson, L. Effects of Simulated N Deposition on Understorey Vegetation of a Boreal Coniferous Forest. *Functional Ecology* **12**, 691–699 (1998).
20. Kahl, S., Gerendás, J., Heeschen, V., Ratcliffe, R. G. & Rudolph, H. Ammonium assimilation in bryophytes. l -glutamine synthetase from *Sphagnum fallax*. *Physiologia Plantarum* **101**, 86–92 (1997).
21. Lockwood, A. L., Filley, T. R., Rhodes, D. & Shepson, P. B. Foliar uptake of atmospheric organic nitrates. *Geophysical Research Letters* **35**, 386–390 (2008).
22. Näsholm, A.-B., Ericsson, A. & Nordén, L. G. Accumulation of amino acids in some boreal forest plants in response to increased nitrogen availability. *New Phytologist* **126**, 137–143 (1994).
23. Näsholm, T. & Ericsson, A. Seasonal changes in amino acids, protein and total nitrogen in needles of fertilized Scots pine trees. *Tree Physiology* **6**, 267–281 (1990).
24. Nussbaum, S. *et al.* Incorporation of atmospheric 15 NO₂ -nitrogen into free amino acids by Norway spruce *Picea abies* (L.) Karst. *Oecologia* **94**, 408–414 (1993).
25. Ohlson, M., Nordin, A. & Näsholm, T. Accumulation of Amino Acids in Forest Plants in Relation to Ecological Amplitude and Nitrogen Supply. *Functional Ecology* **9**, 596–605 (1995).
26. Power, S. A. & Collins, C. M. Use of *Calluna vulgaris* to detect signals of nitrogen deposition across an urban-rural gradient. *Atmospheric Environment* **44**, 1772–1780 (2010).
27. Xu, Y. & Xiao, H. Free amino acid concentrations and nitrogen isotope signatures in *Pinus massoniana* (Lamb.) needles of different ages for indicating atmospheric nitrogen deposition. *Environmental Pollution* **221**, 180–190 (2017).
28. van den Berg, L. J., Peters, C. J., Ashmore, M. R. & Roelofs, J. G. Reduced nitrogen has a greater effect than oxidised nitrogen on dry heathland vegetation. *Environmental Pollution* **154**, 359–369 (2008).
29. Pearson, J. *et al.* Traffic exposure increases natural 15N and heavy metal concentrations in mosses. *New Phytologist* **147**, 317–326 (2000).
30. Skudnik, M., Jeran, Z., Batič, F. & Kastelec, D. Spatial interpolation of N concentrations and δ¹⁵N values in the moss *Hypnum cupressiforme* collected in the forests of Slovenia. *Ecological Indicators* **61**, 366–377 (2016).
31. Boltersdorf, S. H., Pesch, R. & Werner, W. Comparative use of lichens, mosses and tree bark to evaluate nitrogen deposition in Germany. *Environmental Pollution* **189**, 43–53 (2014).
32. Huang, J. *et al.* Urbanization in China changes the composition and main sources of wet inorganic nitrogen deposition. *Environmental Science & Pollution Research International* **22**, 6526–6534 (2014).
33. Liu, X. Y., Koba, K., Liu, C. Q., Li, X. D. & Yoh, M. Pitfalls and new mechanisms in moss isotope biomonitoring of atmospheric nitrogen deposition. *Environmental Science & Technology* **46**, 12557–12566 (2012).
34. Liu, X. Y. *et al.* Ammonium first: natural mosses prefer atmospheric ammonium but vary utilization of dissolved organic nitrogen depending on habitat and nitrogen deposition. *New Phytologist* **199**, 407–419 (2013).
35. Skudnik, M., Jeran, Z. & Kastelec, D. Potential environmental factors that influence the nitrogen concentration and (15)N values in the moss *Hypnum cupressiforme* collected inside and outside canopy drip lines. *Environmental Pollution* **198**, 78–85 (2015).
36. Varela, Z., Carballeira, A., Fernández, J. A. & Aboal, J. R. On the Use of Epigeaic Mosses to Biomonitor Atmospheric Deposition of Nitrogen. *Archives of Environmental Contamination & Toxicology* **64**, 562–572 (2013).
37. Liu, X. Y., Xiao, H. Y., Liu, C. Q., Li, Y. Y. & Xiao, H. W. Atmospheric transport of urban-derived NH(x): Evidence from nitrogen concentration and delta(15)N in epilithic mosses at Guiyang, SW China. *Environmental Pollution* **156**, 715–722 (2008).
38. Gauthier, P. P. *et al.* Metabolic origin of δ¹⁵N values in nitrogenous compounds from *Brassica napus* L. leaves. *Plant Cell & Environment* **36**, 128–137 (2013).
39. Werner, R. A. & Schmidt, H. L. The *in vivo* nitrogen isotope discrimination among organic plant compounds. *Phytochemistry* **61**, 465–484 (2002).
40. Koranda, M., Kerschbaum, S., Wanek, W., Zechmeister, H. & Richter, A. Physiological responses of bryophytes *Thuidium tamariscinum* and *Hylocomium splendens* to increased nitrogen deposition. *Ann Bot* **99**, 161–169 (2007).
41. Bol, R., Ostle, N. J. & Petzke, K. J. Compound specific plant amino acid δ¹⁵N values differ with functional plant strategies in temperate grassland. *Journal of Plant Nutrition & Soil Science* **165**, 661–667 (2002).
42. Xu, Y. & Xiao, H. Concentrations and nitrogen isotope compositions of free amino acids in *Pinus massoniana* (Lamb.) needles of different ages as indicators of atmospheric nitrogen pollution. *Atmospheric Environment* **164**, 348–359 (2017).
43. Yoneyama, T. & Tanaka, F. Natural abundance of 15N in nitrate, ureides, and amino acids from plant tissues. *Soil Science & Plant Nutrition* **45**, 751–755 (1999).
44. Limpens, J. & Berendse, F. Growth reduction of *Sphagnum magellanicum* subjected to high nitrogen deposition: the role of amino acid nitrogen concentration. *Oecologia* **135**, 339–345 (2003).
45. Nordin, A. & Gunnarsson, U. Amino acid accumulation and growth of *Sphagnum* under different levels of N deposition. *Écoscience* **7**, 474–480 (2000).
46. Tomassen, H. B. M. & Roelofs, J. G. M. Stimulated Growth of *Betula pubescens* and *Molinia caerulea* on Ombrotrophic Bogs: Role of High Levels of Atmospheric Nitrogen Deposition. *Journal of Ecology* **91**, 357–370 (2003).

47. Baxter, R., Emes, M. J. & Lee, J. A. Effects of an experimentally applied increase in ammonium on growth and amino-acid metabolism of *Sphagnum cuspidatum* Ehrh. ex Hoffm. from differently polluted areas. *New Phytologist* **120**, 265–274 (1992).
48. Givan, C. V. Metabolic detoxification of ammonia in tissues of higher plants. *Phytochemistry* **18**, 375–382 (1979).
49. Pitcairn, C. E. *et al.* Bioindicators of enhanced nitrogen deposition. *Environmental Pollution* **126**, 353–361 (2003).
50. Wright, K. M. & Givan, C. V. Regulation of non-autotrophic carbon dioxide assimilation by ammonia in cultured cells of *Acer pseudoplatanus* L. *Plant Science* **58**, 151–158 (1988).
51. Chikaraishi, Y. Instrumental optimization for compound-specific nitrogen isotope analysis of amino acids by gas chromatography/combustion/isotope ratio mass spectrometry. *Earth Life & Isotopes*, 367–386 (2010).
52. Richter, C. M., Kranig, S. & Wild, A. Contents of free amino acids in needles of Norway Spruce trees in relation to novel forest decline. Studies on trees from a site in the northern Black Forest. *Environmental Pollution* **87**, 303–312 (1995).
53. Heijden, E. V. D., Verbeek, S. K. & Kuiper, P. J. C. Elevated atmospheric CO₂ and increased nitrogen deposition: effects on C and N metabolism and growth of the peat moss *Sphagnum recurvum* P. Beauv. var. *mucronatum* (Russ.) Warnst. *Global Change Biology* **6**, 201–212 (2000).
54. Styring, A. K., Fraser, R. A., Bogaard, A. & Evershed, R. P. Cereal grain, rachis and pulse seed amino acid $\delta^{15}\text{N}$ values as indicators of plant nitrogen metabolism. *Phytochemistry* **97**, 20–29 (2014).
55. Molero, G., Aranjuelo, I., Teixidor, P., Araus, J. L. & Nogués, S. Measurement of ¹³C and ¹⁵N isotope labeling by gas chromatography/combustion/isotope ratio mass spectrometry to study amino acid fluxes in a plant-microbe symbiotic association. *Rapid Communications in Mass Spectrometry Rcm* **25**, 599–607 (2011).
56. Tcherkez, G. Natural ¹⁵N/¹⁴N isotope composition in C₃ leaves: are enzymatic isotope effects informative for predicting the ¹⁵N-abundance in key metabolites? *Functional Plant Biology* **38**, 1–12 (2011).
57. Felix, J. D., Avery, G. B., Mead, R. N., Kieber, R. J. & Willey, J. D. Nitrogen Content and Isotopic Composition of Spanish Moss (*Tillandsia usneoides* L.): Reactive Nitrogen Variations and Source Implications Across an Urban Coastal Air Shed. *Environmental Processes* **3**, 711–722 (2016).
58. Xiao, H. Y., Tang, C. G., Xiao, H. W., Liu, X. Y. & Liu, C. Q. Mosses Indicating Atmospheric Nitrogen Deposition and Sources in the Yangtze River Drainage Basin, China. *Journal of Geophysical Research Atmospheres* **115**, D14301 (2010).
59. Freyer, H. D. Seasonal trends of NH₄⁺ and NO₃⁻ nitrogen isotope composition in rain collected at Jülich, Germany. *Tellus* **30**, 83–92 (1978).
60. Heaton, T. H. E. ¹⁵N/¹⁴N ratios of NO_x from vehicle engines and coal-fired power stations. *Tellus* **42**, 304–307 (1990).
61. Moore, H. The isotopic composition of ammonia, nitrogen dioxide and nitrate in the atmosphere. *Atmospheric Environment* **11**, 1239–1243 (1977).
62. Cantón, F. R., Suárez, M. F. & Cánovas, F. M. Molecular aspects of nitrogen mobilization and recycling in trees. *Photosynthesis Research* **83**, 265–278 (2005).
63. Smallwood, B. J., Wooller, M. J., Jacobson, M. E. & Fogel, M. L. Isotopic and molecular distributions of biochemicals from fresh and buried *Rhizophora mangle* leaves. *Geochemical Transactions* **4**, 38–46 (2003).
64. Styring, A. K., Fraser, R. A., Bogaard, A. & Evershed, R. P. The effect of manuring on cereal and pulse amino acid $\delta^{15}\text{N}$ values. *Phytochemistry* **102**, 40–45 (2014).
65. Hermes, J., Weiss, P. & Cleland, W. Use of nitrogen-15 and deuterium isotope effects to determine the chemical mechanism of phenylalanine ammonia-lyase. *Biochemistry* **24**, 2959–2967, <https://doi.org/10.1021/bi00333a023> (1985).
66. McClelland, J. W. & Montoya, J. P. Trophic relationships and the nitrogen isotopic composition of amino acids in plankton. *Ecology* **83**, 2173–2180 (2002).
67. Saurer, M., Cherubini, P., Ammann, M., Cinti, B. D. & Siegwolf, R. First detection of nitrogen from NO_x in tree rings: a ¹⁵N/¹⁴N study near a motorway. *Atmospheric Environment* **38**, 2779–2787 (2004).
68. Chikaraishi, Y., Ogawa, N. O., Doi, H. & Ohkouchi, N. ¹⁵N/¹⁴N ratios of amino acids as a tool for studying terrestrial food webs: a case study of terrestrial insects (bees, wasps, and hornets). *Ecological Research* **26**, 835–844 (2011).
69. Hofmann, D., Jung, K., Segsneider, H. J., Gehre, M. & Schüürmann, G. ¹⁵N/¹⁴N Analysis of Amino Acids with GC-C-IRMS - Methodical Investigations and Ecotoxicological Applications. *Isotopes in Environmental & Health Studies* **31**, 367–375 (1995).
70. McCarthy, M. D., Lehman, J. & Kudela, R. Compound-specific amino acid $\delta^{15}\text{N}$ patterns in marine algae: Tracer potential for cyanobacterial vs. eukaryotic organic nitrogen sources in the ocean. *Geochimica Et Cosmochimica Acta* **103**, 104–120 (2013).
71. Paolini, M., Ziller, L., Laursen, K. H., Husted, S. & Camin, F. Compound-Specific $\delta^{15}\text{N}$ and $\delta^{13}\text{C}$ Analyses of Amino Acids for Potential Discrimination between Organically and Conventionally Grown Wheat. *Journal of Agricultural & Food Chemistry* **63**, 5841 (2015).
72. Binder, S., Knill, T. & Schuster, J. Branched-chain amino acid metabolism in higher plants. *Physiologia Plantarum* **129**, 68–78 (2007).
73. Liu, X. Y., Xiao, H. Y., Liu, C. Q. & Li, Y. Y. $\delta^{13}\text{C}$ and $\delta^{15}\text{N}$ of moss *Haplocladium microphyllum* (Hedw.) Broth. for indicating growing environment variation and canopy retention on atmospheric nitrogen deposition. *Atmospheric Environment* **41**, 4897–4907 (2007).
74. Liu, X. Y., Xiao, H. Y., Liu, C. Q., Li, Y. Y. & Xiao, H. W. Stable carbon and nitrogen isotopes of the moss *Haplocladium microphyllum* in an urban and a background area (SW China): The role of environmental conditions and atmospheric nitrogen deposition. *Atmospheric Environment* **42**, 5413–5423 (2008).
75. Zhang, Z., Xiao, H., Zheng, N., Gao, X. & Zhu, R. G. Compound-Specific Isotope Analysis of Amino Acid Labeling with Stable Isotope Nitrogen (¹⁵N) in Higher Plants. *Chromatographia* **79**, 1197–1205 (2016).

Acknowledgements

This study was kindly supported by the National Natural Science Foundation of China through grants 41425014 and 41463007. We thank Gareth Thomas, PhD, from Liwen Bianji, Edanz Group China (www.liwenbianji.cn/ac), for editing the English text of a draft of this manuscript. The authors wish to thank the anonymous referees and the associate editors for helpful comments to improve the paper.

Author Contributions

Ren-guo Zhu conceived and designed the experiments; Ren-guo Zhu, Yuanyuan Lai performed the experiments; Ren-guo Zhu, Hua-Yun Xiao, Zhongyi Zhang analyzed the data; Hua-Yun Xiao contributed reagents or materials or analytical tools; Hua-Yun Xiao, Ren-guo Zhu wrote the paper. All authors reviewed and approved the final version of the manuscript.

Additional Information

Supplementary information accompanies this paper at <https://doi.org/10.1038/s41598-018-32531-x>.

Competing Interests: The authors declare no competing interests.

Publisher's note: Springer Nature remains neutral with regard to jurisdictional claims in published maps and institutional affiliations.



Open Access This article is licensed under a Creative Commons Attribution 4.0 International License, which permits use, sharing, adaptation, distribution and reproduction in any medium or format, as long as you give appropriate credit to the original author(s) and the source, provide a link to the Creative Commons license, and indicate if changes were made. The images or other third party material in this article are included in the article's Creative Commons license, unless indicated otherwise in a credit line to the material. If material is not included in the article's Creative Commons license and your intended use is not permitted by statutory regulation or exceeds the permitted use, you will need to obtain permission directly from the copyright holder. To view a copy of this license, visit <http://creativecommons.org/licenses/by/4.0/>.

© The Author(s) 2018